A finite element and experimental analysis of steady and
unsteady flow over a step

Document status and date:
Published: 01/01/1985

Document Version:
Publisher's PDF, also known as Version of Record (includes final page, issue and volume numbers)

Please check the document version of this publication:

• A submitted manuscript is the version of the article upon submission and before peer-review. There can be
important differences between the submitted version and the official published version of record. People
interested in the research are advised to contact the author for the final version of the publication, or visit the
DOI to the publisher's website.
• The final author version and the galley proof are versions of the publication after peer review.
• The final published version features the final layout of the paper including the volume, issue and page
numbers.

[Link to publication](#)

Download date: 04. Oct. 2023

INTERAFDELINGSPROJECT "ATHEROSCLEROSE".

A finite Element and Experimental Analysis

of Steady and Unsteady Flow over a Step.

F.N.v.d.Vosse

maart 1985

TECHNISCHE HOGESCHOOL EINDHOVEN

contents

1. Introduction

Much research is being done in the field of atherosclerotic disease, a disease which reveals itself as a stiffening and/or narrowing (stenosis) of the arterial vessel. This may lead to partial or full occlusion of the artery lumen and as a consequence to damaging of the tissues that are supplied with blood by this particular vessel. Understanding of the fluid-mechanical properties in both healthy and diseased arteries is of great importance. This is firstly because there are many indications that the genesis of artherosclerosis can be related to regions of distrubed flow like those in bifurcations and bends (Caro et al. 1969, Stehbens 1975, Texon 1976 and Fry 1976). Secondly this is, because understanding of the changes in the flow when stenoses occur may be used for diagnosing the disease in an early stage. To that end the bloodflow velocities and wall displacements can now routinely be obtained by means of ultra-sound Doppler anemometry (Hoeks et al. 1981). A deeper understanding of the complex properties of bloodflow can be obtained by experiments like in vitro velocity measurements (Laser-Doppler anemometry) and by mathematical models. In vitro measurements in models of arteries and artery bifurcations has been performed by several investigators and particularly by Bharadvaj et al. (1982), Zarins et al. (1983) and LoGerfo et al. (1981). Mathematical (i.e. numerical) analysis of blood flow in several models of arterial vessels are reported intensively in the last few years. Gosman et al. (1979) presented numerical solutions of the three-dimensional steady flow in a round pipe with a sector shaped obstacle and used a finite difference method. Wille (1981) used a finite element method to analyse pulsatile pressure and velocity patterns inside an axis symmetric stenosis model and later (1984) presented a finite element formulation for three-dimensional steady flow in a model of the aortic bifurcation. Two-dimensional but pulsating flow analysis in arterial bifurcations are presented by Florian et.al. (1982).

In the present study a mathematical model for unsteady flow in a simplified two-dimensional stenosis model is considered. Mathematical models of blood flow can be obtained by the solution of the well known Navier-Stokes equations. Only for very simple geometries these solutions may follow from analytical calculations. In practice numerical approximation methods like finite difference, discrete vortex or finite element methods are necessary. When dealing with complex (three-dimensional) geometries at relatively low Reynolds numbers (Re < 10^3), the finite element method is the most advantageous because no complex interpolations to incorporate the boundary conditions (see for instance Cebeci et al. 1981) or non-orthogonal body-fitted coordinates (see for instance Gunton et al. 1983) are needed. However, because of the great amount of computing time and memory needed, the solution of the fully three-dimensional unsteady Navier-Stokes equations for complex geometries is very difficult yet. As a preparatory study, in the present paper the attention is focused upon the unsteady Newtonian flow over a rectangular step. The flow behaviour around a step has been the subject of many

investigations. Numerically the studies of Thomas et al. (1981), Hackman et al. (1984) (backward facing steps), Hughes et al. (1979), Leone et al. (1981) and Yang et al. (1984) are closely related to the numerical part of this study. Experimentally the reports of Goldstein et al. (1970), Denham et al. (1974), Mullin et al. (1980), Sinha et al. (1981) and Armaly et al. (1983) are valuable but only deal with backward facing steps.

In section 2 the used numerical method is treated. The finite element equations are derived for a penalty function method and a extended quadratic triangular element. Some attention is payed on time integration schemes that may be used. As a check of the numerical procedure, also the results of some testing examples are given. In section 3 the experimental method is treated with special emphasis to the dataprocessing. In section 4 the results of as well the numerical calculations as the experiments are presented and compared. Finally in section 5 the results are discussed and compared with those obtained from the literature. Some suggestions for further investigation are also given.

2. Numerical method

2.1. General procedure

2.1.1. Finite element discretization of the two-dimensional time-dependent Navier-Stokes equations.

The two-dimensional (2D) Navier-Stokes equations are given by the momentum equations together with the continuity equation (Batchelor, 1967):

$$\varrho \frac{\partial u_i}{\partial t} + \sum_{j=1}^{2} \varrho u_j \frac{\partial u_i}{\partial x_j} = \varrho f_i + \sum_{j=1}^{2} \frac{\partial \sigma_{ij}}{\partial x_j}$$

$$\frac{\partial \varrho}{\partial t} + \sum_{j=1}^{2} \frac{\partial \varrho u_j}{\partial x_j} = 0 \qquad\qquad i=1,2 \qquad (2.1)$$

Where ϱ denotes the density, u_i the i-the component of the velocity, t the time, f_i the volume force per unit mass of fluid in the i-direction and σ_{ij} the Cauchy stress tensor. For a Newtonian fluid, the Cauchy stress tensor reads:

$$\sigma_{ij} = -p\delta_{ij} + \eta(\frac{\partial u_i}{\partial x_j} + \frac{\partial u_j}{\partial x_i}) - \frac{2}{3} \eta \sum_{j=1}^{2} \frac{\partial u_j}{\partial x_j} \qquad (2.2)$$

where p denotes the hydrostatic pressure, δ_{ij} the Cronecker delta and η the dynamic viscosity. In case the fluid is incompressible (i.e. ϱ = constant) the equations reduce to:

$$\varrho \frac{\partial u_i}{\partial t} + \sum_{j=1}^{2} \varrho u_j \frac{\partial u_i}{\partial x_j} = \varrho f_i + \sum_{j=1}^{2} (-\frac{\partial p}{\partial x_j} \delta_{ij} + \frac{\partial}{\partial x_j}[\eta(\frac{\partial u_i}{\partial x_j} + \frac{\partial u_j}{\partial x_i})])$$

$$\sum_{j=1}^{2} \frac{\partial u_j}{\partial x_j} = 0 \qquad\qquad (2.3)$$

The corresponding boundary conditions which specify the considered physical problem and give rise to a unique solution of the problem may be a combination of prescribed velocities and stresses in two independent directions:

$$u_j \text{ or } \sigma_{ij}n_j \text{ prescribed on boundary } \partial\Omega \text{ for } j = 1,2 \qquad (2.4)$$

Note that the pressure is not prescribed on the boundary and can only be prescribed in an explicit way by means of the stress. To solve these equations the Galerkin finite element method is used. The standard method then is to form a weak solution by multiplying equations (2.3) with testfunctions v_i (i=1,2) and q for the momentum and continuity equations respectively and

integrating over the considered domain $d\Omega$:

$$\int_\Omega \left(\frac{\partial u_i}{\partial t} + \sum_{j=1}^{2} u_j \frac{\partial u_i}{\partial x_j}\right) v_i d\Omega = \int_\Omega \left\{f_i - \frac{\partial \hat{p}}{\partial x_i} + \sum_{j=1}^{2} \left(\frac{\partial}{\partial x_j} \left[v\left(\frac{\partial u_i}{\partial x_j} + \frac{\partial u_j}{\partial x_i}\right)\right]\right)\right\} v_i d\Omega$$

$$\int_\Omega \left(\sum_{j=1}^{2} \frac{\partial u_j}{\partial x_j}\right) q \, d\Omega = 0 \qquad\qquad i=1,2 \qquad (2.5)$$

The testfunctions v_i has to be one-time continuously differentiable and q must be integrable. New symbols in the equations (2.5) are $v = \eta/\varrho$, denoted as the kinematic viscosity and $\hat{p} = p/\varrho$. For convenience in the remaining text $\hat{p}$ is denoted as p. Finally integration by parts of the diffusion term and the pressure derivative term in equation (2.5) yields to:

$$\int_\Omega \left(\frac{\partial u_i}{\partial t} v_i + \sum_{j=1}^{2} u_j \frac{\partial u_i}{\partial x_j} q_i\right) d\Omega = \int_\Omega \left\{f_i v_i + p \frac{\partial v_i}{\partial x_i} - \sum_{j=1}^{2} v\left(\frac{\partial u_i}{\partial x_j} + \frac{\partial u_j}{\partial x_i}\right)\frac{\partial v_i}{\partial x_j}\right\} d\Omega$$

$$+ \int_\Gamma \sum_{j=1}^{2} \hat{\sigma}_{ij} n_j v_i d\Gamma \qquad i=1,2$$

$$\int_\Omega \sum_{j=1}^{2} \frac{\partial u_j}{\partial x_j} q \, d\Omega = 0 \qquad\qquad\qquad (2.6)$$

With $\hat{\sigma}_{ij} = \sigma_{ij}/p$ (Also $\hat{\sigma}_{ij}$ is denoted as σ_{ij} in the remaining text). To approximate the unknowns u_i and p, the basisfunctions φ_{in} and ψ_m (n = 1,...,N and m = 1,...,M) are introduced according to:

$$u_i^h = \sum_{n=1}^{N} U_{in} \varphi_{in} \qquad\qquad i=1,2$$

$$p^h = \sum_{m=1}^{M} P_m \psi_m \qquad\qquad\qquad (2.7)$$

Usage of Galerkins method (i.e. $v_{ik} = \varphi_{ik}$, k = 1,...,N and $q_k = \psi_k$, k = 1,...,M) and substitution of the approximations (2.7) in equations (2.6) leads to:

$$\int_\Omega \left(\sum_{n=1}^{N} \dot{U}_{in} \varphi_{in} \varphi_{ik}\right) d\Omega + \int_\Omega \left[\sum_{j=1}^{2} \sum_{n=1}^{N} v\left(U_{in} \frac{\partial \varphi_{in}}{\partial x_j} + U_{jn} \frac{\partial \varphi_{in}}{\partial x_i}\right)\frac{\partial \varphi_{ik}}{\partial x_j}\right] d\Omega +$$

$$+ \int_\Omega \left[\sum_{j=1}^{2} \left(\sum_{n=1}^{N} U_{jn}\varphi_{jn} \sum_{l=1}^{N} U_{il} \frac{\partial \varphi_{il}}{\partial x_j}\right)\varphi_{ik}\right] d\Omega - \int_\Omega \sum_{m=1}^{M} P_m \psi_m \frac{\partial \varphi_{ik}}{\partial x_i} d\Omega =$$

$$\int_\Omega f_i \varphi_{ik} d\Omega + \int_\Gamma \sum_{j=1}^{2} \sigma_{ij} n_j \varphi_{ik} d\Gamma \qquad i=1,2$$
$$k=1,...,N$$

$$-\int_\Omega \sum_{j=1}^{2} \sum_{n=1}^{N} U_{jn} \frac{\partial \varphi_{jn}}{\partial x_j} \psi_k \, d\Omega = 0 \qquad\qquad k=1,...,M$$

$$\qquad\qquad (2.8)$$

This is a set of non-linear ordinary differential equations which can be solved if φ_{in} and ψ_m are prescribed. Before a description of these basis-functions is given, the equations (2.8) are first written in matrix form. Therefore the following matrices are defined:

1. The Mass matrix M (2Nx2N):

$$M = \begin{bmatrix} M^{11} & 0 \\ 0 & M^{22} \end{bmatrix} \qquad M_{kl}^{ii} = \int_{\Omega} \varphi_{ik}\varphi_{il}\,d\Omega \qquad \begin{array}{l} k = 1,\ldots,N \\ l = 1,\ldots,N \\ i = 1,2 \end{array} \qquad (2.9)$$

2. The diffusion matrix S (2Nx2N):

$$S = \begin{bmatrix} S^{11} & S^{12} \\ S^{21} & S^{22} \end{bmatrix} \qquad S_{kl}^{ij} = \int_{\Omega} v\,(\frac{\partial \varphi_{ik}}{\partial x_j} \frac{\partial \varphi_{jl}}{\partial x_i}(1 + \delta_{ij}) + \frac{\partial \varphi_{ik}}{\partial x_j} \frac{\partial \varphi_{il}}{\partial x_j}\delta_{ij})\,d\Omega$$

$$\begin{array}{l} k=1,\ldots,N \\ l=1,\ldots,N \\ ij=1,2 \end{array}$$

$$(2.10)$$

3. The divergence matrix L(Mx2N):

$$L = (L^1\ L^2) \qquad L_{kl}^i = -\int_{\Omega} \psi_k \frac{\partial \varphi_{il}}{\partial x_i}\,d\Omega \qquad \begin{array}{l} k=1,\ldots,M \\ l=1,\ldots,N \\ i=1,2 \end{array}$$

$$(2.11)$$

4. The convection matrix N(U) (2Nx2N):

The convective term is non linear and must be linearized in order to solve the equations in an iterative procedure. If $\underline{U}^v$ is denoted as the solution of the previous iteration simple Picard iteration leads to:

$$N(\underline{U})\underline{U} \rightarrow K(\underline{U}^v)\underline{U}^{v+1}$$

with:

$$K(\underline{U}^v) = \begin{bmatrix} K^1(\underline{U}^v) & 0 \\ 0 & K^2(\underline{U}^v) \end{bmatrix}$$

$$K_{kl}^i(\underline{U}^v) = \sum_{p=1}^{N} \sum_{j=1}^{2} U_{jp} \int_{\Omega} \varphi_{jp}\varphi_{ik} \frac{\partial \varphi_{il}}{\partial x_j}\,d\Omega \qquad \begin{array}{l} k=1,\ldots,N \\ l=1,\ldots,N \\ i=1,2 \end{array}$$

$$(2.12)$$

whereas Newton-Raphson iteration leads to:

$$N(\underline{U})\underline{U} \rightarrow J(\underline{U}^v)\underline{U}^{v+1} - N(\underline{U}^v)\underline{U}^v$$

with
$$J(\underline{U}^v) = \begin{bmatrix} J^{11}(\underline{U}^v) & J^{12}(\underline{U}^v) \\ J^{21}(\underline{U}^v) & J^{22}(\underline{U}^v) \end{bmatrix}$$

$$J^{ij}_{kl} = K^i_{kl} \cdot \delta_{ij} + \sum_{p=1}^{N} U^v_{ip} \int_{\Omega} \frac{\partial \varphi_{ip}}{\partial x_j} \varphi_{ik}\varphi_{jl} d\Omega \qquad \begin{aligned} &k=1,\ldots,N \\ &l=1,\ldots,N \\ &i=1,2 \\ &j=1,2 \end{aligned}$$

$$(2.13)$$

(See appendix 2.1)

5. The force vector $\underline{F}$ (2Nx1):

$$\underline{F} = \begin{bmatrix} \underline{F}^1 \\ \underline{F}^2 \end{bmatrix} \qquad F^i_k = \int_{\Omega} f_i \varphi_{ik} d\Omega \qquad \begin{aligned} &k=1,\ldots,N \\ &i=1,2 \end{aligned}$$

$$(2.14)$$

6. The boundary stress vector $\underline{B}$ (2Nx1):

$$\underline{B} = \begin{bmatrix} \underline{B}^1 \\ \underline{B}^2 \end{bmatrix} \qquad B^i_k = \int_{\Gamma} \sum_{j=1}^{2} \sigma_{ij} n_j \varphi_{ik} d\Gamma \qquad \begin{aligned} &k=1,\ldots,N \\ &i=1,2 \end{aligned}$$

$$(2.15)$$

Together with the definitions 1 to 6 the complete set of non-linearized equations (2.7) may then be written as:

$$M\ddot{\underline{U}} + [S + N(\underline{U})]\underline{U} + L^T\underline{P} = \underline{F} + \underline{B}$$

$$L\underline{U} = 0 \qquad (2.16)$$

2.1.2. The extended quadratic conforming triangular element.

When evaluating the matrices derived in the previous section not any finite element approximation is applicable. The difficulty lies in the treatment of the continuity equation. Of importance in this matter is the so called Babûska-Brezzi condition stating that one cannot mix any velocity approxima-tion with any pressure approximation (Fortin, 1981). An element satisfying this condition is the extended quadratic conforming triangular element des-cribed by Crouzeix and Raviart (1973) with 7 nodal points for the velocity and 1 for the pressure. The velocity is approximated by a quadratic function
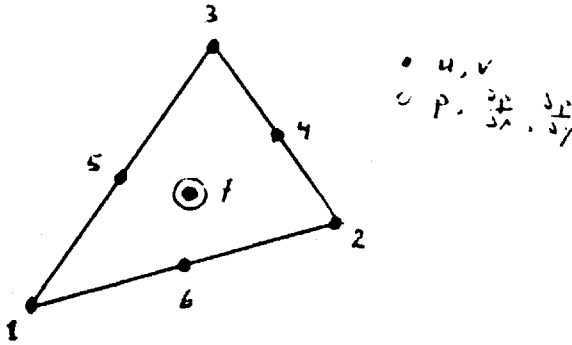
Fig. 2.1.: The extended quadratic conforming triangular element.

plus some third degree terms vanishing at the element boundary. The pressure is approximated linearly by the pressure and its derivatives in the centroid and hereby discontinuous over the boundary elements (see fig. 2.1).

If $\lambda_i(\vec{x})$ are the barycentric coordinates of a point $\vec{x}$ with respect to the vertices of the element (i=1,2,3), the basisfunctions are defined as:

$$\varphi_i = \lambda_i(2\lambda_i-1) + \lambda_1\lambda_2\lambda_3 \qquad 1 \leq i \leq 3$$
$$\varphi_i = 4\lambda_1\lambda_2\lambda_3(1/\lambda_{i-3}-3) \qquad 4 \leq i \leq 6$$
$$\varphi_i = 27\lambda_1\lambda_2\lambda_3 \qquad i=7$$
$$\psi_1 = 1$$
$$\psi_2 = x_1 - x_{1,7}$$
$$\psi_3 = x_2 - x_{2,7} \qquad\qquad\qquad\qquad (2.17)$$

The approximations for velocity and pressure then read:

$$u_i^h = \sum_{n=1}^{7} U_{in} \varphi_{in}$$

$$p^h = p_7\psi_1 + \frac{\partial p}{\partial x_1}\Big|_7 \psi_2 + \frac{\partial p}{\partial x_2}\Big|_7 \psi_3 \qquad\qquad (2.18)$$

Substitution of the foregoing basisfunctions into the equations (2.9 to 2.15) completes the final set of equations (2.16). To carry out these substitutions integrals of the form:

$$\int_\Omega \gamma(\bar{x})d\Omega \quad \text{and} \quad \int_\Gamma \gamma(\bar{x})d\Gamma$$

has to be computed, where γ is an arbitrary function.
To perform these integrations the integrals are written as the sum of the integrals over the elements according to:

$$\int_\Omega \gamma(\bar{x})d\Omega = \sum_{m=1}^{M_e} \int_{\Omega_e} \gamma(\bar{x})d\Omega_e$$

$$\int_\Gamma \gamma(\bar{x})d\Gamma = \sum_{n=1}^{N_e} \int_{\Gamma_e} \gamma(\bar{x})d\Gamma_e$$
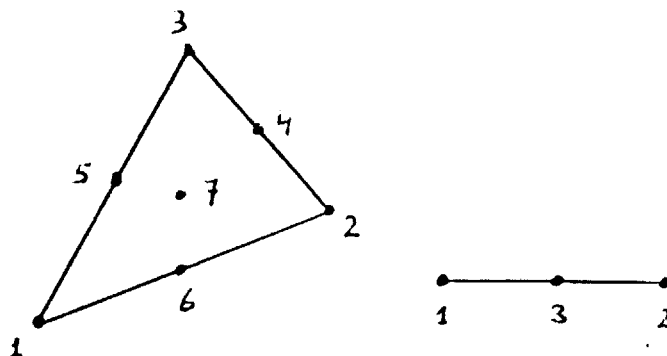

Fig. 2.2. Definition of the nodal point numbers on the element and line element respectively.

where M_e and N_e denote the number of elements and the number of boundary elements (line-elements) respectively. As it is complicated or even impossible to carry out this integrations exactly, numerical integration rules based upon Newton-Côtes formulas are used, which are exact for polynomals γ of degree $\leq$ 3 (Ciarlet, 1978) i.e.:

$$\int_{\Omega_e} \gamma(\bar{x})d\Omega_e = \frac{|e|}{60} \sum_{i=1}^{7} w_{\Omega i}\, \gamma_i$$

$$\int_{\Gamma_e} \gamma(\bar{x})d\Gamma_e = \frac{|e|}{6} \sum_{i=1}^{3} w_{\Gamma i}\, \gamma_i$$

where $|e|$ denotes the absolute value of the "volume" of the element and

$$w_{\Omega i} = \begin{cases} 3 & \text{for } i=1,2,3 \\ 8 & \text{for } i=4,5,6 \\ 27 & \text{for } i=7 \end{cases}$$

$$w_{\Gamma i} = \begin{cases} 1 & \text{for } i=1,2 \\ 4 & \text{for } i=3 \end{cases}$$

(see fig. 2.2)   (2.19)

Together with the basisfunctions defined by equation (2.17) an error estimate of $O(h^3)$ for the velocity and $O(h^2)$ for the pressure is expected (Crouzeix-Raviart, 1973). The extended quadratic element with 17 unknowns (14 velocities and 3 pressure parameters) may be modified by eliminating the velocities and the pressure derivatives in the centroids. Then the number of unknowns per element is reduced to 13. This is ofcourse advantageous with respect to memory and computing time usage. To elucidate this elimination process the discrete but not yet linearised Navier-Stokes equations are

again considered:

$$M\dot{\underline{U}} + S\underline{U} + N(\underline{U})\underline{U} + L^T\underline{P} = \underline{F}+\underline{B} \tag{2.20}$$
$$L\underline{U} = 0$$

Next the velocity $\underline{U}$ is splitted in a part $\hat{\underline{U}}$ containing the velocity para-
meters in the vertices and midpoints of the sides of the element (length $\hat{\underline{U}}$:
$2N - 2M/3$) and a part $\underline{U}_c$ containing the velocity parameters in the centroids
(length $\underline{U}_c$: $2M/3$). Analougously the pressure parameters can be splitted in a
part $\underline{P}_c$ containing the pressure values in the centroid (length $M/3$) and a
part $\underline{P}_\nabla$ containing the pressure derivative parameters (length $2M/3$). After
the elimination process evaluated in appendix 2.2 equation (2.20) changes
into:

$$\hat{M}\dot{\hat{\underline{U}}} + [\hat{S} + \hat{N}(\underline{U})]\hat{\underline{U}} + \hat{L}^T\underline{P}_c = \hat{\underline{F}} + \hat{\underline{B}}$$
$$\tag{2.21}$$
$$\hat{L}\,\hat{\underline{U}} = 0$$

with:

$$\underline{U}_c = R_0\,\hat{\underline{U}}$$

$$\hat{A} = A_{11} + A_{12}R_0 + R_0^T A_{22}R_0 \qquad\qquad \hat{A} = \hat{M},\;\hat{S},\;\hat{N}$$

$$\hat{L} = L_{11}$$

$$\hat{\underline{C}} = [I_0^T \; R_0^T]\underline{C} \qquad\qquad \hat{\underline{C}} = \hat{\underline{F}},\;\hat{\underline{B}}$$

and:

$$R_0 = -L_{22}^{-1}\,L_{21}$$

$$I_0 = I \quad (2N-2M)\times(2N-2M)$$

$$A\underline{U} = \begin{bmatrix} A_{11} & A_{12} \\ A_{21} & A_{22} \end{bmatrix} \begin{bmatrix} \hat{\underline{U}} \\ \underline{U}_c \end{bmatrix} \qquad A = M,S,N,L \tag{2.22}$$

The pressure derivatives can be recovered elementwise by means of:

$$\underline{P}_\nabla = (L_{22}^T)^{-1}\,[\underline{F}_c - (M_{22}R_0 + S_{21} + N_{21}(\underline{U}) + S_{22}R_0 + N_{22}(\underline{U})R_0)]\hat{\underline{U}} \tag{2.23}$$

(see appendix 2.2).

2.1.3. Descretisation of the time derivative

Now the treatment of the time derivative terms in the discrete Navier-Stokes equations (2.21) is focused.
They are approximated here by a finite difference θ-method. Considering the equation:

$$\dot{\underline{U}} = \underline{f}$$

this approximation is defined by:

$$\frac{\underline{U}^{n+1} - \underline{U}^{n}}{\Delta t} = \underline{f}^{\theta}$$

with $\underline{f}^{\theta} = \theta \, \underline{f}^{n+1} + (1-\theta)\underline{f}^{n}$ $0 \leq \theta \leq 1$ (2.24)

For $\theta = 0$ and $\theta = 1$ this scheme reduces to the Euler explicit and Euler implicit method respectively, which are both $O(\Delta t)$ accurate for linear equations. For $\theta = 0.5$ the scheme becomes the Crank-Nicolson scheme which is of $O(\Delta t^2)$ accurate for linear equations.

To choose a θ-value preferable for the solution of the Navier-Stokes equations a closer look to time integrations for parabolic equations is necessary. Therefore the following parabolic equation is considered:

$$\dot{\underline{U}} = A\underline{U} + \underline{f}$$

with initial condition $\underline{U}(t_0) = \underline{U}_0$.   (2.25)

Here A is assumed to be a NxN matrix with real coefficients only depending on time. For convenience A is assumed to be non-defect, which means that A has N linear independent eigenvectors. If A is a defect matrix the situation is more complicated but the same properties of the time integrations considered here can be derived. In the former case, due to the N linear independent eigenvectors a non-singular matrix S exists with complex coefficients defined by:

$$AS = S\Lambda$$ (2.26)

with $\Lambda = \text{diag}(\lambda_1, \ldots, \lambda_N)$ and $\lambda_1, \ldots, \lambda_N$ the N eigenvalues of A. The differential equation (2.25) but also its discretized approximation is now called stable when a finite error $\underline{\varepsilon}_0$ in the initial condition $\underline{U}_0$ results in a finite error in $\underline{U}(t)$, for any t. To evaluate this error propagation two cases are considered:

1. $\underline{U}$ is a solution of (2.25) with $\underline{U}(t_0) = \underline{U}_0$.
2. $\underline{\xi}$ is a solution of (2.25) with $\underline{\xi}(t_0) = \underline{U}_0 + \underline{\varepsilon}_0$ with $\underline{\varepsilon}_0$ a small pertubation on $\underline{U}_0$.

If $\underline{\varepsilon}$ is defined as $\underline{\varepsilon} = \underline{\xi} - \underline{U}$ then $\dot{\underline{\xi}} = A \underline{\varepsilon}$ and $\underline{\varepsilon}(t_0) = \underline{\varepsilon}_0$. Besides, S is non-singular and hence a vector $\underline{n} = S^{-1}\underline{\varepsilon}$ exists. This leads to the set of equations:

$$S\dot{\underline{n}} = AS\underline{n}$$

or

$$\dot{\underline{n}} = \Lambda\underline{n}$$

with initial value

$$\underline{n}(t_0) = S^{-1}\underline{\varepsilon}_0 \equiv \underline{n}_0 \qquad (2.27)$$

As Λ is a diagonal matrix it may also be written as:

$$\dot{n}_i = \lambda_i n_i$$
$$n_i(t_0) = n_{i0} \qquad\qquad\qquad i=1,\ldots,N$$

with solution:

$$n_i = n_{i0}e^{\lambda_i(t-t_0)} \qquad (2.28)$$

For stability the pertubations may not increase, hence a necessary condition for stability is:

$$Re(\lambda_i) \leq 0 \quad \text{for any } i \qquad (2.29)$$

Numerical time integration schemes of (2.25) generally lead to equations for $\underline{n}$ of the form:

$$\underline{n}^{n+1} = G\underline{n}^n \qquad (2.30)$$

with G the so called amplification matrix and $\underline{n}^n = \underline{n}(t_n)$. To require stability of the numerical scheme it is necessary that $||G|| \leq 1$ (with $||G||$ for instance the maximum norm defined as $||G|| = \max \sum_{j=1}^{N} |G_{ij}|$).
To evaluate the stability of the θ-method of time integration equation (2.24) is rewritten in the form:

$$\frac{\underline{n}^{n+1}-\underline{n}^n}{\Delta t} = \theta\Lambda\underline{n}^{n+1} - (1-\theta)\Lambda\underline{n}^n$$

or

$$[I - \theta\Delta t\Lambda]\underline{n}^{n+1} = [I + (1-\theta)\Delta t\Lambda]\underline{n}^n \qquad (2.31)$$

For stability it is necessary that

$$||[I - \theta\Delta t\Lambda]^{-1}[I + (1-\theta)\Delta t\Lambda]|| < 1$$

So for any λ_i ($i=1,\ldots,N$), the next equation must hold:

$$|c| \equiv |\frac{1+(1-\theta)\lambda_i\Delta t}{1-\theta\lambda_i\Delta t}| < 1 \tag{2.32}$$

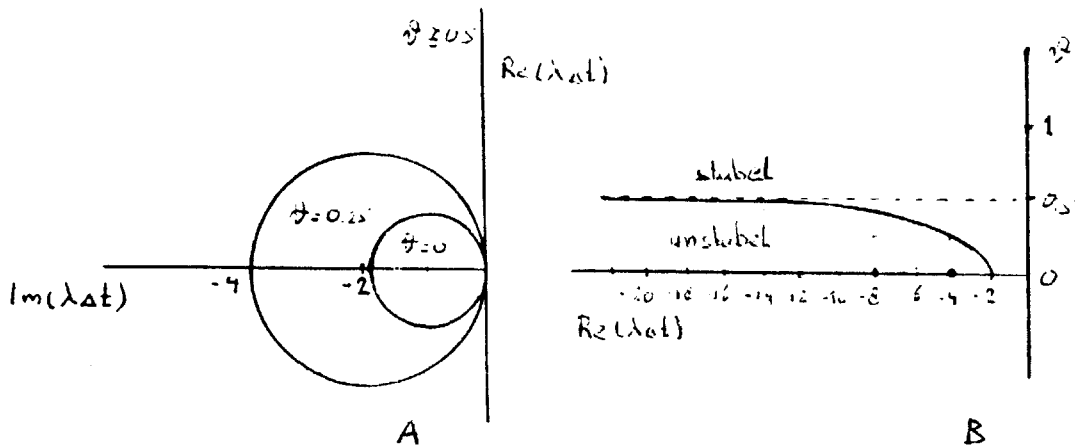In fig. 2.3 the stability areas of $\lambda_i\Delta t$ are given for the interval $0 \le \theta \le 1$.

Fig. 2.3: A: Stability regions of $\lambda_i\Delta t$ for $v = 0$, 0.25, 0.5
B: Stability condition for Re($\lambda\Delta t$) as a function of θ.

For $0.5 \le \theta \le 1$ the scheme appears to be stable for all $\lambda\Delta t$. For $0 \le \theta < 0.5$ the scheme is conditionally stable. In case the eigenvalues are large a relative small timestep Δt has to be choosen to ensure stability. In that case integration with $\theta > 0.5$ is preferable. The amplificationfactor c is also calculated as a function of $\lambda\Delta t$ for $\theta = 0.5$ and $\theta = 1$ respectively, the results of which are given in figures 2.4 and 2.5.
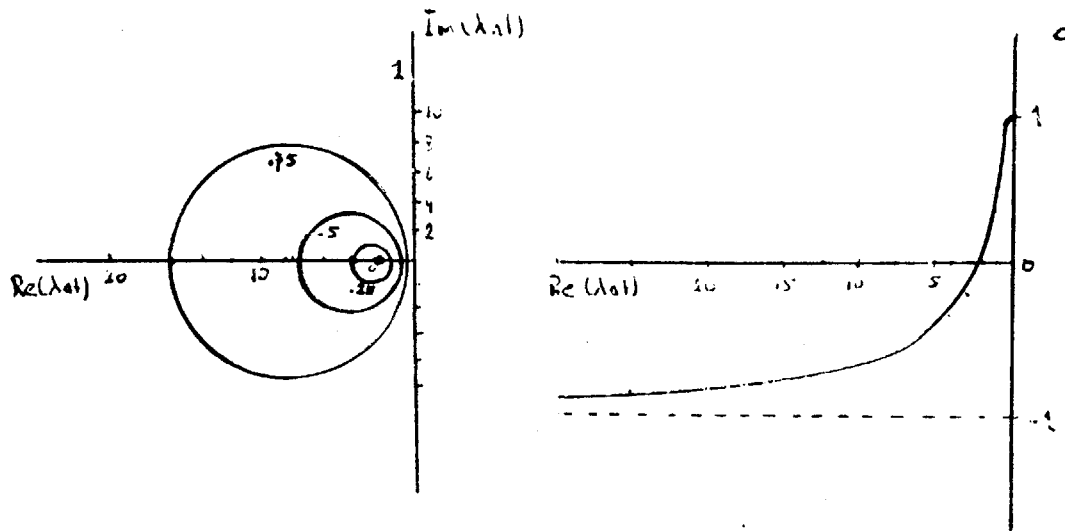
Fig. 2.4: Lines of c = constant in the complex ($\lambda\Delta t$)-plane and amplification factor c as a function of Re($\lambda\Delta t$) for θ = 0.5.
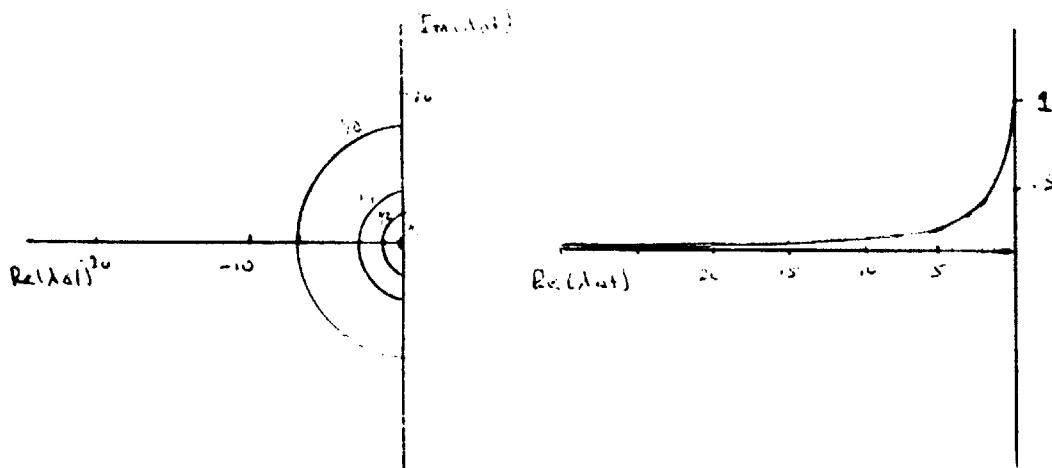

Fig. 2.5: Lines of c = constant in the complex ($\lambda\Delta t$)-plane and amplification factor c as a function of Re($\lambda\Delta t$) for θ = 1.

From fig. 2.4 and 2.5 it is concluded that for θ = 0.5 (Crank Nicolson) the amplification tends to unity for Re($\lambda\Delta t$) $\rightarrow$ 0 and tends to minus one for Re($\lambda\Delta t$) $\rightarrow$ $-\infty$ whereas for θ = 1.0 (Euler implicit) the amplification only tends to unity only for Re($\lambda\Delta t$) $\rightarrow$ 0.
To indicate whether one method is preferable to the other the eigenvalues of the system that has to be solved has to be known. In case these eigenvalues (or some of them) are relatively high and the Crank-Nicolson scheme is used a very slow damping of calculation errors or errors in the initial condition is expected, in contrast to the Euler implicit scheme where this damping will be very fast. When using a penalty function method as explained in the

next section the largest eigenvalues are of order $1/\varepsilon$ while ε is a very small parameter. Due to the small value of ε one may expect that consequently error's in the initial value will only damp very slowly when the Crank-Nicolson scheme is used. Therefore, an implicit scheme may be preferable for the first few time-steps.

2.1.4. Penalty formulation of the unsteady Navier-Stokes equations

After finite element discretisation the non-linearised unsteady Navier-Stokes equations may generally be written in the form:

$$M\dot{\underline{U}} + [S+N(\underline{U})]\underline{U} + L^T\underline{P} = \underline{F} + \underline{B}$$

$$LU = \underline{O}$$

(2.33)

Application of the θ-method of time integration described in the previous sections gives:

$$\{M + \theta\Delta t[S+N(\underline{U}^{n+1})]\}\underline{U}^{n+1} + \theta\Delta tL^T\underline{P}^{n+1} = \Delta t(\underline{F}^\theta+\underline{B}^\theta) +$$

$$+ \{M - (1-\theta)\Delta t[S+N(\underline{U}^n)]\}\underline{U}^n - (1-\theta)\Delta tL^T\underline{P}^n$$

$$L\underline{U}^{n+1} = \underline{O}$$

(2.34)

Direct solution of this set of equations has a great disadvantage because of the zero-elements appearing on the principle diagonal of the coefficient matrix, hence a partial pivoting procedure is demanded by which the bandstructure is disturbed resulting in not only a time consuming but also a memory consuming procedure. This all is a consequence of the fact that the pressure does not occur in the continuity equation. To overcome this difficulty, the finite element method is not applied directly to the Navier-Stokes equations (2.3) but to equations in which the continuity is perturbed and replaced by:

$$\sum_{j=1}^{2} \frac{\partial u_j}{\partial x_j} = -\varepsilon p$$

(2.35)

where ε, the penalty parameter, stands for a small (i.e. εp is small) parameter. This pertubation has no direct physical meaning but is a consequence of the Lagrange multiplier method for constrained minimization problems, where the Lagrange multiplier is observed to be the negative of the pressure (Reddy, 1982). For the steady Navier-Stokes equations it is proved that the solution of the penalty problem converges to the solution of the original problem as ε approximates zero. Theoretical analysis by Reddy (1982) show that for the steady Stokes equation a convergence order exists of $O(\varepsilon^{-1})$ while at least an order of $O(\varepsilon^{-1/2})$ exists for the Navier-Stokes equation. Numerical analysis showed a convergence rate of 1 for both cases (Reddy, 1982). The main advantage of the penalty method over the direct method is,

that the pressure p is eliminated from the momentum equation. The pressure is then obtained, after the perturbed momentum equation is solved, from the velocity.

We now apply the penalty function method to the modified extended quadratic element described in section 2.12. The continuity equation (eq. 2.21) then changes into:

$$\ddot{L}\underline{\ddot{U}} = \epsilon \hat{M}_p \underline{\hat{P}}_C$$

with

$$\hat{M}_p = \int_\Omega \psi_1 \, d\Omega \qquad\qquad (2.36)$$

Substitution in the other equations of the set (2.21) yields:

$$\hat{M}\underline{\ddot{U}} + [\hat{S}+\hat{N}(\underline{U}) + \sigma \hat{L}^T \hat{M}_p^{-1} \hat{L}]\underline{\ddot{U}} = \underline{\hat{F}} + \underline{\hat{B}}$$
$$\underline{P}_C = \frac{1}{\epsilon}\hat{M}_p^{-1} \hat{L} \, \underline{U}$$

$$\underline{U}_C = R_0 \, \underline{\hat{U}}$$

$$\underline{P}_V = (L_{22}^T)^{-1}[\underline{\hat{F}}_C - \{M_{22}R_0 + S_{21} + N_{21}(\underline{U}) + S_{22}R_0 + N_{22}(\underline{U})R_0\}]\underline{\ddot{U}}$$

$$(2.37)$$

Now the momentum equation and the continuity equation are uncoupled and no partial pivoting is necessary. Also the number of unknowns in the equations to be solved are decreased. (Due to the diagonal matrix M_p, the pressure can be obtained from the velocity by a simple matrix-vector multiplication). Using the θ-method for time integration changes equation (2.37) into:

$$\hat{M} + \theta\Delta t[\hat{S}+\hat{N}(\underline{U}^{n+1}) + \frac{1}{\epsilon}\hat{L}^T\hat{M}_p^{-1}\hat{L}]\}\underline{\hat{U}}^{n+1} = \Delta t(\underline{\hat{F}}^\theta + \underline{\hat{B}}^\theta) +$$

$$+ \{\hat{M} - (1-\theta)\Delta t[\hat{S}+\hat{N}(\underline{U}^n) + \frac{1}{\epsilon}\hat{L}^T\hat{M}_p^{-1}\hat{L}]\}\underline{\hat{U}}^n$$

$$\underline{P}_C^{n+1} = \frac{1}{\epsilon}\hat{M}_p^{-1} \hat{L}\underline{U}^{n+1}$$

$$\underline{U}_C^{n+1} = R_0\underline{\hat{U}}^{n+1}$$

$$\underline{P}_V^\theta = (L_{22}^T)^{-1} [\underline{\hat{F}}_C^\theta - \{\frac{1}{\Delta t}M_{22}R_0 + \theta[S_{21}+N_{21}\underline{U}^{n+1}) + S_{22}R_0 + N_{22}(\underline{U}^{n+1})R_0]\}\underline{\hat{U}}^{n+1}$$

$$-\{\frac{1}{\Delta t} M_{22}R_0 + (1-\theta)[S_{21} + N_{21}(\underline{U}^n) + S_{22}R_0 + N_{22}(\underline{U}^n)R_0]\}\underline{\hat{U}}^n]$$

$$(2.38)$$

A main disadvantage of this method regards the penalty parameter ϵ. Too large values of this parameter leads to inaccurate results. However, too small values cause a worsening of the condition of the coefficient matrix

and hence difficulties with regard to the stability and convergence of the time integration may be expected.

## 2.5. The final set of equations

Analogously to eq. (2.16) the non-linear convective term $N(\underline{U}^{n+1})\underline{U}^{n+1}$ in eq. (2.38) has to be linearized, before the equations can be solved. When the timesteps are taken to be that small that one single Newton step is sufficient to linearize the equations with the desired accuracy, the linearization of the unsteady Navier-Stokes equations reduces to:

$$\hat{N}(\underline{U}^{n+1})\underline{U}^{n+1} = \hat{J}(\underline{U}^n)\underline{U}^{n+1} - \hat{N}(\underline{U}^n)\hat{\underline{U}}^n \qquad (2.39)$$

The complete linear set of equations then read:

$$\hat{M} + \theta\Delta t[\hat{S}+\hat{J}(\underline{U}^n) + \tfrac{1}{\varepsilon}\hat{L}^T M_p^{-1}\hat{L}]\}\hat{\underline{U}}^{n+1} = \Delta t(\hat{\underline{F}}^\theta + \hat{\underline{B}}^V) +$$

$$+ \{\hat{M} - (1-\theta)\Delta t[\hat{S}+\tfrac{1}{\varepsilon}\hat{L}^T M_p^{-1}\hat{L}]\}\hat{\underline{U}}^n - (1-2v)N(\underline{U}^n)\hat{\underline{U}}^n$$

$$\underline{P}_C^{n+1} = \tfrac{1}{\varepsilon}\hat{M}_p^{-1}\hat{L}\underline{U}^{n+1}$$

$$\underline{U}_C^{n+1} = R_0\hat{\underline{U}}^{n+1}$$

$$\underline{P}_V^\theta - (L_{22}^T)^{-1}[\underline{F}_C^\theta - \{\tfrac{1}{\Delta t} M_{22}R_0 + \theta[S_{21}+N_{21}(\underline{U}^{n+1}) + S_{22}R_0 +$$

$$+ N_{22}(\underline{U}^{n+1})R_0]\}\hat{\underline{U}}^{n+1} +$$

$$-\{\tfrac{1}{\Delta t} M_{22}R_0 + (1-\theta)[S_{21}+N_{21}(\underline{U}^n) + S_{22}R_0 + N_{22}(\underline{U}^n)R_0]\}\hat{\underline{U}}^n$$

Finally, it is remarked that the pressure changes discontinous from element to element. An estimation of the pressure in the vertices can be obtained by averaging the values of all aligning elements in each vertex (see fig. 2.6).
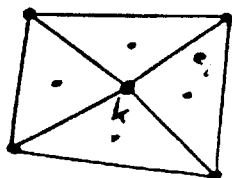
$$P_k = \tfrac{1}{4} \sum_{i=1}^{4} \sum_{j=1}^{3} P_j\psi_j(\bar{x}_j)$$

Fig. 2.6 Averaging of the pressure.

2.2. Testing examples

2.2.1. The steady Navier-Stokes equations

For steady solutions of the Navier-Stokes equations the penalty approach (2.40) reduces to:

$$[\hat{S}+\hat{J}(\underline{U}^v) + \frac{1}{\varepsilon}\hat{L}^T\hat{M}_p^{-1}\hat{L}]\underline{U}^{v+1} = \hat{F} + \hat{B} + N(\underline{U}^v)\underline{U}^v \qquad v=0,1,\ldots,v_m$$

$$\underline{P}_c^v = \frac{1}{\varepsilon}\hat{M}_p^{-1}\hat{L}\underline{U}^v$$

$$\underline{U}_c^v = R_0\hat{\underline{U}}^v$$

$$\underline{P}_v^v = (L_{22}^T)^{-1}[\underline{F}_c - [S_{21} + N_{21}(\underline{U}^v) + S_{22}R_0 + N_{22}\underline{U}^v)R_0]\underline{U}^v$$

$$(2.42)$$

where v_m denotes the maximum number of iterations. The iteration procedure is terminated when $||\underline{U}^v - \underline{U}^{v-1}||_{max} < \varepsilon$ ($\varepsilon = 10^{-4}$). To evaluate the order of accuracy the problem as depected in fig. 27 is analysed in which the body forces are taken to be equal to:

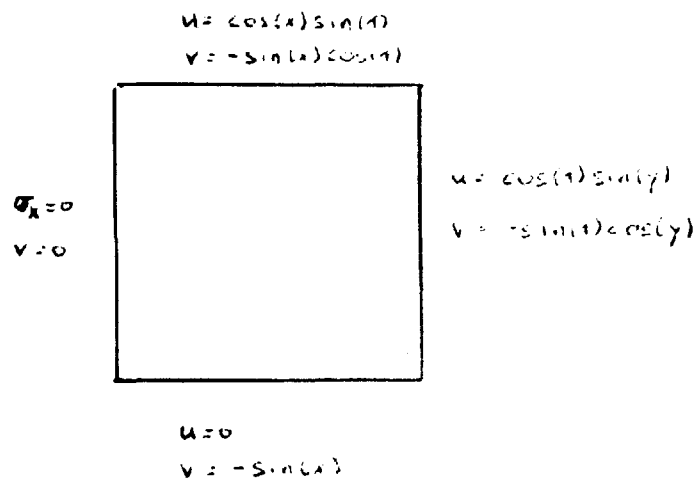$$f_1 = 3v \cos x \sin y$$

$$f_2 = -v \sin x \cos y \qquad (2.43)$$

Fig. 2.7 Testing example time-independent equations.